Prehistoric Wall-Paintings Reconstruction Using Image Pattern Analysis And Curve Fitting

Th. Panagopoulos, C. Papaodysseus*, M. Exarhos, C. Triantafillou, G. Roussopoulos, P. Roussopoulos
School of Electrical and Computer Engineering,
National Technical University of Athens,
9 Heroon Polytechneiou, GR-15773, Athens,
GREECE

Abstract: In the Greek island of Thera extraordinary wall-paintings dated from 1650 B.C.are excavated in many thousands of widely scattered fragments whose depiction manifests inhomogeneous colour decay, odd texture, cracks, added extraneous material etc. In this paper a colour image segmentation method as well as a pattern analysis in connection with these wall-paintings, are presented. The colour image segmentation method takes into account these problems and eventually offers very satisfactory, clear-cut and precise colour regions and region borders for each fragment depiction. Extensive pattern analysis to the obtained regions borders leads to the conclusion that 3650 years ago, the artist most probably used advanced geometrical methods in order to construct handcrafted "French curves" (stencils or templates) and use them to draw certain figures. On the basis of the above results, specific pattern matching techniques are employed for the reconstruction of wall-paintings depicting spirals, from their constituent fragments.

Key-Words: - Image Segmentation, Pattern Matching, Curve Fitting, Archaeological Image Processing

1 Introduction

The discovery of the wall-paintings at Akrotiri of the Greek island Thera (Santorini), is of outstanding importance for human knowledge of the early Aegean world and not only. According to prominent archaeologists these wall-paintings rank alongside the greatest archaeological discoveries. The late professor Marinatos originated the excavations, which are now continued by Professor Christos Doumas. The wall-paintings of Thera were preserved due to the seal of the pumice from the great eruption of a volcano [1]. As a rule the walls decorated with paintings collapsed together with their painted coat before the volcanic eruption, due to particularly strong earthquakes. Thus, a single painting is usually scattered into many fragments mixing with the fragments of other wall-paintings too. The restoration of the wall-paintings from the fragments is very painstaking and time consuming process. Therefore, the development of a system that will contribute to the automatic reconstruction of these wall-paintings is of fundamental importance for this archaeological research, but for many others too, which face the problem of an image reconstruction from excavated fragments. If one wishes to develop such a system, one may take into account many parameters, such as a) matching between external contours of the fragments ([9]) b) region borders continuation between actually adjacent fragments c) colour continuation d) continuation of the thematic content e) crack continuation f) geological texture of the side opposite to the painted one, etc.

For parameters b), c), d) above, it is absolutely necessary and essential to automatically extract as clear-cut and precise as possible colour regions and region borders from each fragment. For this reason, employing an efficient colour image segmentation method is absolutely critical. There are numerous publications dealing with the problem of segmenting a greyscale or colour image using various techniques such as split and merge [2], watershed [3], and other ([4], [5]). In addition, there are other particularly useful publications evaluating such methods [6]. Since each fragment is characterized by inhomogeneous colour decay, odd texture, presence of cracks, added extraneous material etc, it has been necessary to develop a colour image segmentation method specifically oriented to achieve an as clear-cut and accurate as possible fragment region and region borders extraction. We would like to point out that the originality of the developed method lies mainly on the employed sequence of already existing partial techniques, their variation, as well as the proper choice of the used parameters. The developed segmentation method is equally well applicable to other cases than the present archaeological application, too.

Detailed inspection of the fragments depiction gave us the feeling that the artist 1650 years B.C. used

prototypes to draw parts of the wall-paintings. Therefore, the developed segmentation method and the obtained clear-cut boundaries have been extensively used:

1. To unambiguously spot and describe models used by the artist and
2. To achieve corresponding wall paintings parts reconstruction.

In connection with curve fitting, various publications exist, using statistical methods, parameterized families of polynomials, parametric deformable models, simplicial models, normalized primitives ([7], [8]) etc.

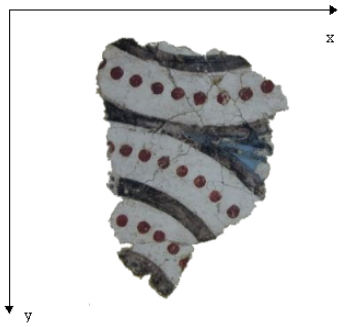

Figure 1

2 Colour Image Segmentation Method

More than four thousand (4000) fragments belonging to several wall-paintings, have been, for the first time, photographed and "extracted" using the methodology described in [9]. The fragments digital images are stored in a database and processed for quality improvement.

The initial fragment positioning together with axes is considered to be "the absolute reference system" for each fragment separately, in all subsequent analysis (see Figure 1).

2.1 An initial colour region extraction

First, one defines the notion of "decay noise", which describes the random colour and texture decay that has occurred to the fragment in hand. A simple method to calculate this decay noise is the following: One transforms the initial fragment coloured image into a grey scale one and computes the resulting intensity "finite gradient" $G_f(i,j)=|\Delta_x|+|\Delta_y|=|I(i+1)-I(i)|+|I(j+1)-I(j)|$ at each fragment pixel (i,j). Next, one computes the mean value E_G and the root mean square R_G of $G_f(i,j)$ and checks the number of pixels N_G that lie in the interval $(E_G-R_G,\ E_G+R_G)$. If N_G is less than a considerable percentage P_G ($P_G=0.8$ for the application in hand) of the total number of fragment pixels N, then one considers that a serious degree of decay noise exists and so a 9x9 pixels mask is used in order to achieve image colour smoothing.

Subsequently, we define a proper multidimensional colour histogram and obtain its maxima as follows: We estimate the minimum and maximum value of each colour component R, G, B for all fragment image pixels, say $R_m, R_M, G_m, G_M, B_m, B_M$ and we divide each one of the intervals $[R_m,R_M]$, $[G_m,G_M]$, $[B_m,B_M]$ into p subintervals $S_X^i, i=1,2,...,p,\ X=R,G,B$ of length $l_X=(X_M-X_m)/p$. We consider the Cartesian product of all these one-dimensional intervals, thus obtaining a three dimensional partition of the parallelepipedon $[R_m,R_M]\times[G_m,G_M]\times[B_m,B_M]$. Next, we classify all fragment image pixels into these 3-d intervals in a straightforward manner. Notice, that the value $p=32$, offered very good results for all the available fragments.

Subsequently, we count the number of pixels $M_{i,j,k}$ belonging to each cell $I_{i,j,k}$ and we spot the local maxima of $M_{i,j,k}$, $i,j,k=1,2,...,p$ that include, however, a number of pixels greater than a certain threshold TH_M. For the present application and the chosen image analysis we have set $TH_M=100$. For each such local maximum, say at (a,b,c) we consider the "extended" cell $E_{C(a,b,c)}=\bigcup_{i=a-1}^{a+1}\bigcup_{j=b-1}^{b+1}\bigcup_{k=c-1}^{c+1} I_{i,j,k}$.

We consider that the ensemble of pixels belonging to this "extended" cell is a first rude approximation of an image region. Notice, that with this procedure one obtains a class of regions $E_{C(i,j,k)}$ that are possibly overlapping but they do not necessarily cover the entire colour image.

Subsequently, we make the plausible assumption that, in a unique colour region, the colour variations may be considered as random variables following a normal distribution. Based on this assumption, one can extend the previously defined regions by means of the following procedure:

1. One computes the mean value μ_X and the root mean square σ_X, $X=R,G,B$ of the three colour components R,G,B in every previously defined set of pixels $E_{C(i,j,k)}$.
2. Since the decisively greatest part of a normal distribution population lies in the three-dimensional interval

$J=[\mu_R-3.12\sigma_R,\ \mu_R+3.12\sigma_R]\times[\mu_G-3.12\sigma_G,\ \mu_G+3.12\sigma_G]\times$ the $[\mu_B-3.12\sigma_B,\ \mu_B+3.12\sigma_B]$

n, one extends the region $E_{C(i,j,k)}$, to a broader one including all pixels having colour components in $J_{(i,j,k)}$.

The above procedure generates a class of broader regions $J_{(i,j,k)}$, which are still, most probably, overlapping.

The final goal is to classify each image pixel into a single region. In order to do so, first one, quite classically, defines a distance d of a pixel P with colour components R_P, G_P, B_P, from an arbitrary region U with mean values μ_X, $X=R,G,B$ of its pixels colour components R,G,B, via the formula:

$d_{(P,U)}=|(\mu_R-R_P)|+|(\mu_G-G_P)|+|(\mu_B-B_P)|$.

Now, if a pixel is classified to more than one region, say $U_1,U_2,\ldots,U_n$ via the previous process, one attributes this pixel to the region from which it has the minimum distance, i.e. $d_{(P,U_k)}=\min_{j=1,\ldots,n}\{d_{(P,U_j)}\}\Rightarrow P\in U_k$.

With the same method, one attributes to a certain region all pixels that have not been classified to any region during the process of section 2.2.

Finally, in every pixel of the fragment image one assigns a colour content equal to the average values μ_X, $X=R,G,B$ of the region the pixel belongs to. In this way, one obtains a "first homogenised approximation" of the fragment image.

2.2 Decay noise reduction and edge refining

After dividing the fragment image into regions and obtaining the "homogenised" fragment image one uses the procedure described below to reduce decay noise:

A $m\times n$ mask, m and n odd, slides throughout the whole fragment image each time centred at a pixel P of it. At each mask position one counts the number of pixels of the mask perimeter belonging to each defined region separately. Let U_M be the region with the greater number of perimeter pixels, say N_M. If N_M is greater than a percentage, say $\Pi_{m,n}$ of the number of the mask perimeter pixels, then all mask pixels are assigned to region U_M. The aforementioned procedure is continually repeated, until no mask pixel assignment is reported. Next, then mask dimensions are reduced by 2 and the whole process is repeated until m=n=3.

The above procedure eliminates the decay noise in the internal of each region successfully. However, a certain amount of decay noise still remains in the regions borders. In order to reduce this decay noise too, one may apply the following:

A $m\times n$ mask, m and n odd, slides throughout the whole fragment image each time centred at a pixel P of it. At each mask position one counts the number of mask pixels belonging to each defined region separately and let $U_{\max}$ and $U_{\min}$ be the regions with the greater and smaller number of pixels respectively, say $N_{\max}$, $N_{\min}$. Then one checks if the following conditions are satisfied:

1. The mask centre belongs to the region $U_{\min}$.
2. $N_{\min}$ is smaller than a percentage, say $\Pi_{\min(m,n)}$ of the number of the mask pixels.
3. $N_{\max}$ is greater than a percentage, say $\Pi_{\max(m,n)}$ of the number of the mask pixels.

If so, the central pixel of the mask is assigned to region $U_{\max}$. The aforementioned procedure is continually repeated, until no mask pixel assignment is reported. Next, then mask dimensions are reduced by 2 and the whole process is repeated until m=n=3.

Notice, that there is an intimate relation between the degree of decay noise the fragments have suffered and the proper values of the thresholds $\Pi_{m,n}$, $\Pi_{\min(m,n)}$ and $\Pi_{\max(m,n)}$. After estimating the decay noise of all available fragments we have set $\Pi_{m,n}=0.7$, $\Pi_{\min(m,n)}=0.25$ and $\Pi_{\max(m,n)}=0.5$.

Figure 2

In this way, one obtains the "final homogenised" fragment image (see Figure 2). If one wants to obtain an even more homogenised segmentation one may repeat the smoothing procedure referred to in section 2.1 to each obtained region separately, where, however, the initial colour content of the region pixels is used. The outcome of this procedure is once more subjected to the aforementioned segmentation process. At this point the primary goal, namely a clear-cut "final border" extraction, can be immediately accomplished by a direct application of any respectable edge detection algorithm, as well as any boundary extraction one, to the final

homogenized fragment image. Examples of the obtained very satisfactory results are shown in Figure 3.

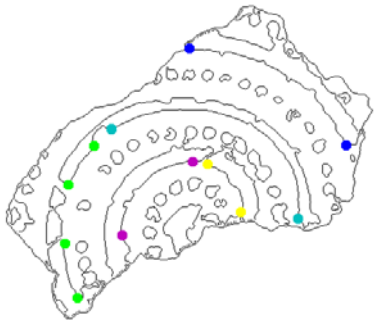

Figure 3

3 Spotting Various Geometrical Shapes - Estimation Of The Mathematical Models

At first, we have observed that some thematic areas boundaries belong to well known geometrical shapes like straight lines, circles, spirals, crescents etc. We have observed too, that all geometrical shapes parts depicted on numerous fragments are smooth and manifest noticeable similarities. This imposed the idea that the artist, 1650 years B.C., used specific geometrical methods and/or templates to draw these geometrical shapes. To test this conjecture we have tried to find proper mathematical functions describing these shapes.

At this point, employing clear-cut boundaries of these geometrical shapes is absolutely essential. Such boundaries parts are extracted from the final borders of the homogenized segmented image (Figure 3). The most difficult and interesting related problem is the demonstration that all found spiral parts depicted in numerous fragments belong to specific spiral models. In order to tackle this problem we have proceeded as follows:

It is well known that the general spiral equation is of the form:

$x(\theta)=x_0+R(\theta)*\cos(\alpha(\theta)),\ y(\theta)=y_0+R(\theta)*\sin(\alpha(\theta))$

where $R(\theta)$ is any increasing function of θ , (x_0, y_0) the spiral centre coordinates and $\alpha(\theta)$ is any function of θ. If the parameters of the model spiral are $a_1, a_2,..., a_n$ and if the actual spiral part is a curve (x_i, y_i), we recursively find the proper values of the parameters $a_i\ i=1,...,n$ that make a specific model part best fit in the Least Squares sense to (x_i, y_i).

In this way we have tested if the drawn spirals correspond to a number of prototype spirals that for which, from the archaeological point of view, one cannot exclude the possibility that the artist was capable of constructing them by means of a geometrical method:

1. Archimedes spiral, namely $R(\theta)=k*\theta$, and $\alpha(\theta)=\theta-\phi_0$, where ϕ_0 accounts for a possible spiral rotation.
2. The spiral that corresponds to unwrapping a thread wrapped around a nail, with equation

$x(\theta)=x_0+r_0\sqrt{1+\theta^2}*\cos(\theta-\arctan(\theta))$,

$y(\theta)=y_0+r_0\sqrt{1+\theta^2}*\sin(\theta-\arctan(\theta))$

3. The logarithmic spiral with $R(\theta)=a*e^{\beta*\theta}$, $\alpha(\theta)=\theta-\phi_0$, where α, β are constants and ϕ_0 accounts for a possible spiral rotation.

After applying this method to all available actually drawn spiral parts we have reached the following conclusions:

a) Model spirals 2 and 3 poorly approximate the drawn spirals.

b) The prototype linear (Archimedes) spiral with $\kappa=23.69$ very well approximates all the actually drawn parts of the large class presented in this paper. The approximation becomes excellent if one makes the assumption, fully compatible with all the archaeological observations so far, that the artist had divided the initial linear spiral prototype into “French curves” (stencils or templates) in order to draw the spirals (see Figure 4).

Figure 4

The aforementioned conclusion may be used to fit the many hundreds of wall-paintings fragments depicting these spirals to their proper position as uniquely as possible. It seems that the novel method described below is the most appropriate for reconstructing the wall-paintings from their constituent parts even if no conduct between the various fragments exists [9].

4 Fitting Fragments Into Specific Models

In this section, a general methodology is chosen to fit a part to a proper model. Consider two curves in the same

plain, say (x_i, y_i) and (P_i, Q_i) respectively, of equal length, say N pixels, with arbitrary orientation. Suppose that one wants to estimate the optimum rotation and parallel translation so as to fit curve (x_i, y_i) to curve (P_i, Q_i) in the Least Squares sense. In other words, one wants to estimate the proper angle of rotation θ and (x_0, y_0) so if,

$$Y_i = y_0 + y_{i*}\cos(\theta) + x_{i*}\sin(\theta)$$

$$X_i = x_0 - y_{i*}\sin(\theta) + x_{i*}\cos(\theta)$$

then quantity

$$E = \sum_{all\ i}\left\{(X_i - P_i)^2 + (Y_i - Q_i)^2\right\}$$

is minimum. After derivation and some straightforward calculus one obtains:

$$x_0 = \frac{1}{N} * \sum_{i=1}^{N}(P_i - \delta x_i),\quad y_0 = \frac{1}{N} * \sum_{i=1}^{N}(Q_i - \delta y_i)$$

$$\tan(\theta) = \frac{\sum_{i=1}^{N}(x_i * \delta Q_i - y_i * \delta P_i)}{\sum_{i=1}^{N}(x_i * \delta P_i + y_i * \delta Q_i)},$$

where $\delta x_i = -y_{i*}\sin(\theta) + x_{i*}\cos(\theta)$

$$\delta y_i = y_{i*}\cos(\theta) + x_{i*}\sin(\theta)$$

$$\delta P_i = \frac{1}{N}\sum_{j=1}^{N} P_j - P_i\ ,\ \delta Q_i = \frac{1}{N}\sum_{j=1}^{N} Q_j - Q_i\ .$$

Finally, one obtains the pixel n where $E(n)$ becomes minimum and this is the starting position of the model spiral where the internal boundary part best fits.

One may extend the aforementioned technique to fit many internal boundaries – spiral parts of a fragment to the same single or double spiral model. In other words, if many spiral parts are depicted on the very same fragment, then one may simultaneously fit all the corresponding internal boundaries to a spiral model. To set ideas, suppose that on a certain fragment two internal boundaries are depicted belonging to different spiral parts, say $(x_{1,i}, y_{1,i})$ and $(x_{2,i}, y_{2,i})$, where, one arbitrarily defines one of the spiral parts as #1 and the other #2. At this point, one computes the distance δ of the beginnings A=$(x_{1,0}, y_{1,0})$ and B=$(x_{2,0}, y_{2,0})$ of spiral parts #1 and #2, as well as the angle ϕ_0 between vector $\overrightarrow{AB}$ and the tangent to the first spiral part at point A (see Figure 5) and performs the following steps, in order to fit $(x_{1,i}, y_{1,i})$, $(x_{2,i}, y_{2,i})$ to a double spiral model:

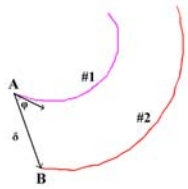

Figure 5

1. For every pixel n_1 of the model spiral, one generates a N_1 pixel arc, say C_{n1}, starting from pixel n_1 where N_1 is the length of #1 actual spiral part.
2. One spots all pixels $m_{1,i}$ of the model spiral having a distance $\delta \pm \varepsilon$ from pixel n_1 and such that each vector $(n_{1,i}, m_{1,i})$ forms an angle $\phi_0 \pm \xi$ with the tangent to the spiral model at point n_1 where, ε, ξ small, properly chosen, scalar quantities.
3. For every such pixel $m_{1,i}$ of the model spiral, one generates a N_2 pixel arc, say $C_{m1,i}$, starting from pixel $m_{1,i}$ where N_2 is the length of #2 actual spiral part.
4. For every such pixel $m_{1,i}$ one forms the "extended" model spiral arc $\Gamma_{n1,i}$ of length $N_1 + N_2$ where its first N_1 points are the pixels of curve C_{n1}, while the last N_2 points are the pixels of curve $C_{m1,i}$.
5. Similarly, one has already defined the "extended" actual spiral boundary arc, say A_E which is formed by a concatenation of spiral parts $(x_{1,i}, y_{1,i})$ and $(x_{2,i}, y_{2,i})$. Once more, the first N_1 points of A_E are the pixels of boundary spiral part $(x_{1,i}, y_{1,i})$, while the last N_2 points are the pixels of $(x_{2,i}, y_{2,i})$.
6. Subsequently, for every pair of curves A_E and $\Gamma_{n1,i}$ one applies the previously described method, namely one computes angle of rotation θ and (x_0, y_0) via equations (4.4) and (4.5) that offer the Least Squares difference $E(n_1, i)$ of A_E and $\Gamma_{n1,i}$.
7. Finally, one obtains the couple of pixels (n_1, i) where $E(n_1, i)$ becomes minimum and these are the starting positions of the model spiral where the internal boundaries $(x_{1,i}, y_{1,i})$ and $(x_{2,i}, y_{2,i})$ best fit simultaneously.

Figure 6

In order to fit more than two internal boundaries – spiral parts simultaneously into a spiral model, one applies the aforementioned procedure by creating extended arcs A_E and $\Gamma_{n1,i,j,\ldots,m}$ consisting of more than two actual or model spiral parts.

Application of the method introduced above, allowed the reconstruction of all wall-paintings parts consisting of fragments with spiral parts depicted on them (see Figures 6,7,8). Finally, we would like to point out that the methodology introduced here is actually applied to reconstructing wall-paintings from its constituent fragments by fitting depicted figures to other prototypes, e.g. ellipses, parallel lines grids, too.

Figure 7

Figure 8

5 Conclusion

A colour image segmentation method as well as a pattern analysis has been presented, in connection with the extraordinary 1650 B.C. wall-paintings of the Greek island of Thera, excavated in many thousands of widely scattered fragments suffering a serious decay. The introduced colour image segmentation method takes into account the decay problems and offers clear-cut colour regions and region borders for each fragment depiction. Extensive pattern analysis to the obtained regions borders leads to the conclusion that 3650 years ago, the artist most probably used advanced geometrical methods in order to construct handcrafted prototypes or "templates" and use them to draw certain figures. On the basis of the above results, specific pattern matching techniques are employed for the reconstruction of wall-paintings depicting spirals, from their constituent fragments.

References

[1] C. Doumas, "The Wall-Paintings of Thera", The Thera Foundation P. Nomikos, Kapon Editions, 1999

[2] Y. L. Chang and X. Li, "Adaptive image region-growing", IEEE Trans. on Image Processing, Vol. 3, 1994, pp. 868-872

[3] T. Gevers and A. W. M. Smeulders, "Combining region splitting and edge detection through guided Delaunay image subdivision", IEEE Computer Society Computer Vision and Pattern Recognition, 1997, pp. 1021-1026

[4] Hung-Hsin Chang and Hong Yan, "Vectorization of hand-drawn image using piecewise cubic Bezier curves fitting", Pattern Recognition 31, 11-1998, pp 1747-1755

[5] K.C. Yao, M. Mignotte, C. Collet, P. Galerne and G. Burel, "Unsupervised segmentation using a self-organizing map and a noise model estimation in sonar imagery" Pattern Recognition 33, 9-2000, pp 1575-1584

[6] R. Román-Roldán, J.F. Gómez-Lopera, C. Atae-Allah, J. Martínez-Aroza and P. L. Luque-Escamilla, "A measure of quality for evaluating methods of segmentation and edge detection", Pattern Recognition 34, pp. 969-980, 5-2001

[7] M. Werman and D.Keren, "A Bayesian Method for Fitting Parametric and Nonparametric Models to Noisy Data", IEEE Transactions on Pattern Analysis and Machine Intelligence, (Vol. 23, No. 5), May 2001

[8] D. Craig, "Fitting Curves and Surfaces With Constrained Implicit Polynomials", IEEE Transactions on Pattern Analysis and Machine Intelligence, (Vol. 21, No. 1), January 1999, pp. 31-41

[9] C. Papaodysseus, Th. Panagopoulos, M. Exarhos, C. Triantafyllou, D. Fragoulis, "Contour-shape Based Reconstruction of Fragmented, 1600 B.C. Wall Paintings", IEEE Transactions on Signal Processing, (Vol. 50, No 6), pp.1277-1288, June 2002.